

CHARACTERISATION OF CASCADED ARC THERMAL PLASMA SOURCE IN ARGON AND HYDROGEN: EXPERIMENT AND MODELLING

Zhou Qing¹, D.K. Otorbaev^{1,2}, E.B. Kulumbaev², V.F. Semenov²,
V.M. Lelevkin², M.C.M. van de Sanden¹ and D.C. Schram¹

¹Department of Physics, Eindhoven University of Technology,
P.O. Box 513, 5600 MB Eindhoven, The Netherlands,

²Laboratory of Plasma Spectroscopy, Kyrgyz National Academy
of Sciences, Chui prospect 265 A, Bishkek, 720071, Kyrgyzstan.

A cascaded arc plasma source in argon and hydrogen has been experimentally characterized by determination of the efficiency, the electric field, and the pressure gradient. The experimental data were in a good agreement with the results of numerical modelling, based on the two-dimensional magnetohydrodynamic conservation equations of continuity, momentum and energy, and the Maxwell equations.

INTRODUCTION

Thermal plasmas, as plasma torches and inductively coupled plasmas have become very important for many industrial applications as plasma spraying, powder processing, high pressure light sources and spectrochemistry. More recently plasma deposition (etching) with thermal plasmas and with a cascaded arc in particular, is proven to offer great advantages in terms of effectiveness of the process and hence of the deposition (etching) rate [1]. For the applications a good control of the plasma properties as temperature fields, ionization and dissociation degree and flow velocity is crucial. The cascaded arc is an example of a wall stabilized thermal plasma and can be operated in a wide range of pressures and currents. As a simple and stable plasma source it has already been widely used both in fundamental research of non-equilibrium and non-ideal effects in plasmas, and in applications. To obtain a thorough knowledge of the cascaded arc, to optimize the design of the arc setup and to find new efficient regimes of arc operation, further experimental and theoretical investigations are required.

EXPERIMENT

The cascaded arc used consist of three cathodes, an anode plate with a nozzle and several copper cascaded plates. The total length of the arc was either 30 or 60 mm, the diameter of the arc channel was 4 mm. Experimentally, the determination of the axial parameters of the arc has been realized by electric potential measurements, cooling water flow temperature and arc pressure measurements. The electric potential of each component of the arc was measured by a voltage divider. To measure the pressure in a cascaded arc, small holes to the central channel (diameter of 2 mm) were drilled at each of cascaded plates. The exit of the holes was connected to a calibrated pressure sensor. Generally speaking the measured pressure reflects the pressure of the arc plasma at the wall position. The cooling water temperature was measured by a calibrated semiconductor temperature sensor, the flow of the cooling water by a water flow transmitter.

The electric field at a position z along the arc channel is given by:

$$E(z) = \frac{j(z)}{\sigma[n_e(z), T_e(z)]}, \quad (1)$$

where $j(z)$ is the current density, and σ is the electrical conductivity of the plasma. The well-known Frost mixing rule [2] provides a numerical relation between T_e and σ .

The efficiency of the cascaded arc is defined as the fraction of the input power which is converted into plasma generation. Since the elements of the arc were water cooled, in the stationary state the power loss at a position i equals, neglecting the radiation loss, the power used in heating the cooling water.

MODELLING

The flow of the cascaded arc plasma in a cylindrical channel with an axial gas flow is considered. It is assumed that the plasma is stationary, that the flow has cylindrical symmetry, that it is subsonic and laminar, that the radiation is emitted from the whole volume of the plasma. In equilibrium approximation the magnetohydrodynamical (MHD) conservation equations of continuity, momentum, energy, the Maxwell equations, and the Ohm's law may be written in terms of cylindrical coordinates:

$$\begin{aligned} \frac{1}{r} \frac{\partial}{\partial r}(\rho v r) + \frac{\partial}{\partial z}(\rho u) &= 0, \\ \rho v \frac{\partial v}{\partial r} + \rho u \frac{\partial v}{\partial z} &= -\frac{\partial p}{\partial r} - j_z B_\varphi + \frac{2}{r} \frac{\partial}{\partial r} \left(r \eta \frac{\partial v}{\partial r} \right) - \\ &- \frac{2\eta v}{r^2} + \frac{\partial}{\partial z} \left[\eta \left(\frac{\partial u}{\partial r} + \frac{\partial v}{\partial z} \right) \right] - \frac{\partial}{\partial r} \left[\frac{2}{3} \eta \left(\frac{1}{r} \frac{\partial r v}{\partial r} + \frac{\partial u}{\partial z} \right) \right], \end{aligned}$$

$$\begin{aligned}
\rho v \frac{\partial u}{\partial r} + \rho u \frac{\partial u}{\partial z} &= -\frac{\partial p}{\partial z} + j_r B_\varphi + 2 \frac{\partial}{\partial z} \left(\eta \frac{\partial u}{\partial z} \right) + \\
&+ \frac{1}{r} \frac{\partial}{\partial r} \left[r \eta \left(\frac{\partial u}{\partial r} + \frac{\partial v}{\partial z} \right) \right] - \frac{\partial}{\partial z} \left[\frac{2}{3} \eta \left(\frac{1}{r} \frac{\partial r v}{\partial r} + \frac{\partial u}{\partial z} \right) \right], \quad (2) \\
\rho v C_p \frac{\partial T}{\partial r} + \rho u C_p \frac{\partial T}{\partial z} &= j_r E_r + j_z E_z - \psi + \frac{1}{r} \frac{\partial}{\partial r} \left(r \lambda \frac{\partial T}{\partial r} \right) + \frac{\partial}{\partial z} \left(\lambda \frac{\partial T}{\partial z} \right) + v \frac{\partial p}{\partial r} + \\
+ u \frac{\partial p}{\partial z} + 2\eta &\left[\left(\frac{\partial v}{\partial r} \right)^2 + \left(\frac{\partial u}{\partial z} \right)^2 + \left(\frac{v}{r} \right)^2 + \frac{1}{2} \left(\frac{\partial u}{\partial r} + \frac{\partial v}{\partial z} \right)^2 \right] - \frac{2}{3} \eta \left(\frac{1}{r} \frac{\partial r v}{\partial r} + \frac{\partial u}{\partial z} \right)^2, \\
\frac{\partial E_r}{\partial z} - \frac{\partial E_z}{\partial r} &= 0, \quad \frac{1}{r} \frac{\partial}{\partial r} (r B_\varphi) = \mu_0 j_z, \quad \frac{\partial B_\varphi}{\partial z} = -\mu_0 j_r. \\
j_r &= \sigma (E_r - u B_\varphi), \quad j_z = \sigma (E_z + v B_\varphi).
\end{aligned}$$

The system of equations have been solved by a method described in detail elsewhere [3]. The main system of equations is extended by the equation of state, by the dependencies of the transport coefficients on the temperature and pressure, and boundary conditions [3].

RESULTS AND DISCUSSION

Both experiments and calculations have been performed for the cascaded arc in pure argon and in pure hydrogen. The experiments have been carried out for the arc current 50 A, however the calculations have been made in the broader range of the arc currents, as well as for the various percentage of the gas mixture argon-hydrogen. Two different regimes of cascaded arc operation have been investigated: 1) regime with a gas flow rate $Q = 3.5$ slm, and 2) regime with a relatively low gas flow rate $Q = 0.5 - 1$ slm. In these two regimes the pressure in the arc varies from sub-atmospheric in the first regime, to a few tenths of mbar in the second.

Figs. 1, 2 illustrates the temperature fields (in 10^3 K units) and the lines of electric current for the argon and hydrogen arc in the first regime of operation. It can be seen that the characteristics of the thermal arc in hydrogen differs significantly from that in argon for similar arc settings. In contrast to the argon arc, near the axis of the hydrogen arc a sharp radial temperature gradient occurs: a strongly constricted high-temperature axial channel is realized. However the axial values of T_e^{max} were approximately the same both for argon and for hydrogen, i.e. ≈ 13 000 K. Because of high thermal conductivity of H_2 fast cooling of the gas is taking place. Close to the channel walls, the ionization and dissociation degrees of hydrogen plasma are much lower than the axial values; the only flow of neutral hydrogen molecules occur. It has been shown, that in the hydrogen arc the conductive heat flux on the walls of the channel exceeds the heat flux in the argon arc by more than order of magnitude for similar arc parameters.

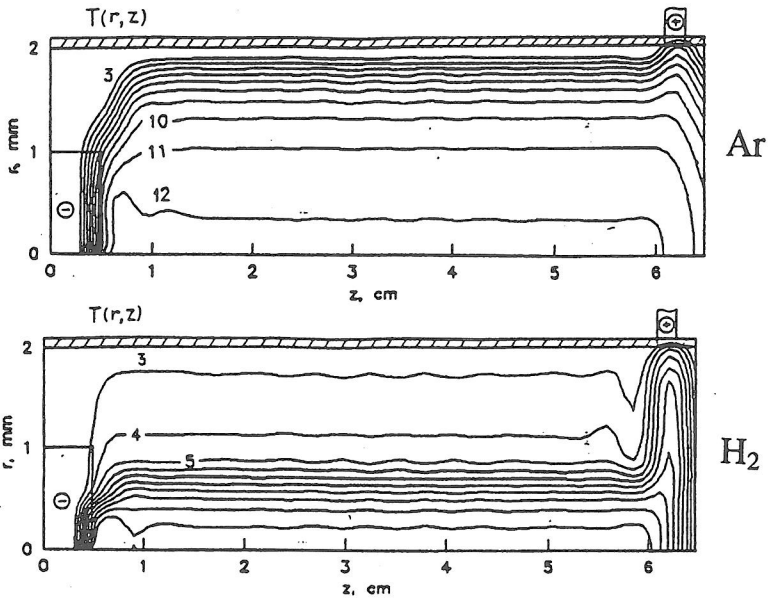


Fig. 1

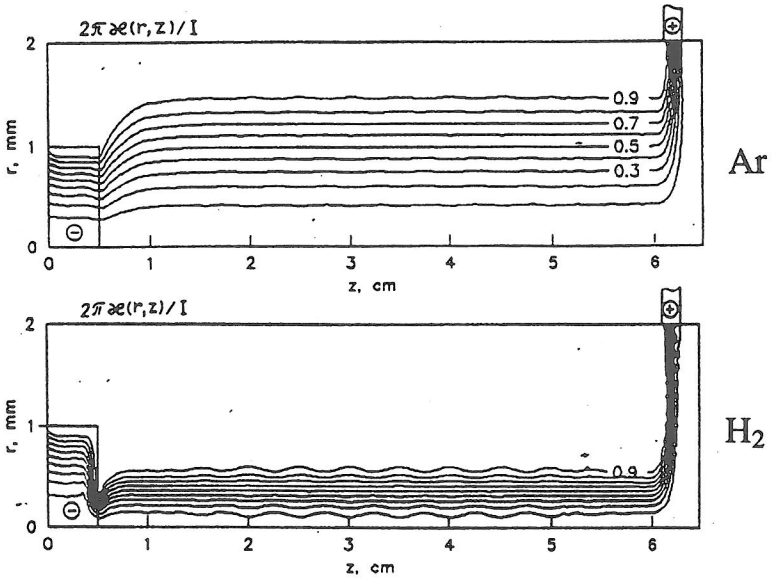


Fig. 2

The results of comparison of the experimental data on the pressure and electric field behaviour along the axis of the cascaded arc with the calculations are shown in Figs. 3,

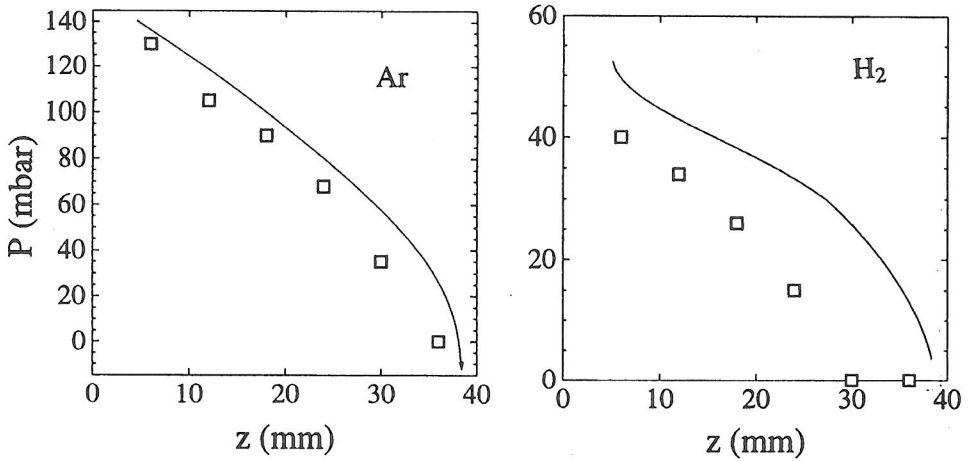


Fig. 3

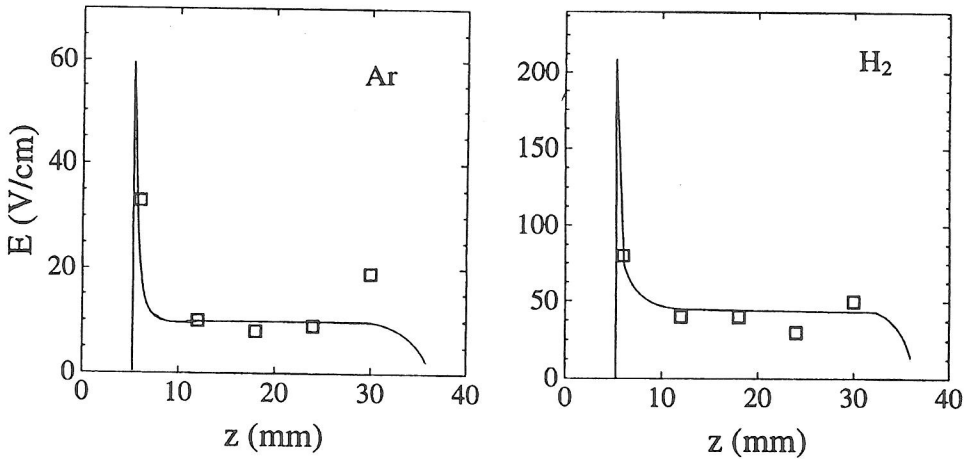


Fig. 4

4 (regime with a low gas flow). For the electric field it can be seen good agreement between the experiment and the calculations, however the calculated gas pressure was

systematically higher, than the experimentally observed (the effect is stronger for the hydrogen plasma). The reason for the observed discrepancy, we believe, is connected with the equilibrium approximation, which was used during the calculation of the chemical composition of the low-pressure plasma. Indeed, as it has been shown the discrepancy becomes smaller in the regime with a larger gas flow, where the equilibrium approximation can in principle be used.

The experimental results as well as the calculations show that efficiency of the hydrogen arc are lower than the same characteristic of the arc in argon. From the power balance and electric field measurements an average electron temperature for the argon arc has been determined. The results of measurements were in a good agreement with the calculations (Fig. 1). The same procedure, applied to the T_e determination of hydrogen plasma, allow us to estimate quantitatively the effect of constriction (narrowing of the arc channel) of the hydrogen plasma. From the power balance and electric field measurements and calculated T_e , the effective radius of the hydrogen plasma can be derived. It has been shown, that the effective radius for the hydrogen arc was approximately two times smaller, than for the argon arc. These observations are in a good agreement with the theoretical calculations (Figs. 1, 2). The dissociation of the hydrogen molecules in the small gas flow range ($Q \simeq 0.5$ slm) was almost complete, whereas in the larger gas flow region it is drops monotonically with increasing the flow. It can be concluded, that besides the pressure in the arc, the results of numerical modelling on efficiency, electric field strength and electron temperature of the cascaded arc were in good agreement with the experimental data both for hydrogen and argon plasma. This means that the discussed numerical code could be used for a quantitative description and optimization of the parameters of thermal plasma. For the low gas flow (low pressure) regime the possibility of supersonic expansion of the plasma in the arc channel should be discussed, besides the non-equilibrium kinetics should be introduced in order to determine the real chemical composition of the plasma.

ACKNOWLEDGEMENTS

This work was partially supported under grant No. 713-224 of Netherlands Organization for Scientific Research (NWO), and partially supported under grant No. 94-2922 of INTAS.

REFERENCES

1. G.M.W. Kroesen, C.J. Timmermans and D.C. Schram, *Pure & Appl. Chem.* **60**, 795 (1988).
2. Zhou Qing, M.J. de Graaf, M.C.M. van de Sanden, D.K. Otorbaev and D.C. Schram, *Rev. Sci. Instrum.* **65**, 1469 (1994).
3. V.M. Lelevkin, D.K. Otorbaev and D.C. Schram, *Physics of Non-Equilibrium Plasmas* (Amsterdam, Elsevier, 1992).